Influencing the homing and differentiation of MNCs in hereditary hemorrhagic telangiectasia

Dingenouts, C.K.E.

6

Endoglin deficiency alters the epicardial response following myocardial infarction

Calinda K.E. Dingenouts[1*&], Asja T. Moerkamp[1*], Kirsten Lodder[1], Tessa van Herwaarden[1], Anna M. D. Végh[1], Esther Dronkers[1], Boudewijn P.T. Kruithof[1], Karien C. Wiesmeijer[1], Janita A. Maring[1], Helen M. Arthur[2], Marie-José Goumans[1#†], Anke M. Smits[1#†]

1. Department of Cell and Chemical Biology, Leiden University Medical Center, Leiden, the Netherlands.
2. Institute of Genetic Medicine, Newcastle University, International Centre for Life, Newcastle upon Tyne, United Kingdom.

*/# Both authors contributed equally
&Current address: Department of Infectious Diseases, Leiden University Medical Center, Leiden, the Netherlands.

Manuscript in submission

Introduction

The epicardium is a dynamic epithelial layer covering the surface of the heart. It plays a critical role in heart formation by differentiating into cardiovascular cell types and providing paracrine factors to the developing myocardium [9]. In the adult heart, upon myocardial infarction (MI) the dormant epicardial layer is reactivated and supports the underlying myocardium during repair [24, 34, 40]. The epicardial response to injury includes upregulation of a developmental gene program, such as re-expression of Wilms' tumour 1 (WT1), proliferation, thickening of the epicardial layer and covering of the damaged myocardium [15, 43, 44]. Furthermore, the epicardial cells undergo epithelial to mesenchymal transition (EMT), thereby forming epicardial-derived cells (EPDCs) that contribute to endogenous repair [34, 40]. Decreased expansion of the epicardial layer and minimal collagen deposition in the (sub)epicardial region, suggesting deficient EMT, result in ventricular dilatation and impaired cardiac function [13]. As such, epicardial EMT is important for a 'healthy' epicardial post-injury response.

The transforming growth factor beta (TGFβ) signaling pathway plays a key role in epicardial EMT. *In vitro*, stimulation of EPDCs with TGFβ results in loss of their epithelial character and induces transition into a mesenchymal phenotype [5, 35]. TGFβ exerts its effect via phosphorylation of the transcription factors small mothers against decapentaplegic 2/3 (SMAD2/3) or SMAD1/5 [18]. These downstream mediators of the TGFβ pathway are upregulated in the epicardial region upon MI [44]. The TGFβ co-receptor endoglin plays an important role in defining the balance between these two TGFβ-responsive pathways resulting in different behavioral outcomes [11, 19]. Mice heterozygous for the TGFβ co-receptor endoglin (*Eng*+/-) display a reduced cardiac function post-MI suggesting that endoglin is important in the cardiac response to injury [26]. Endoglin is well known for its expression in activated endothelial cells and its essential role during angiogenesis [11]. Endoglin knockout embryos die around embryonic day 10.5 due to vascular abnormalities [3, 7, 30]. However, it is becoming clear that the role of endoglin goes beyond maintenance of vascular homeostasis and, for example, also affects the immune response to injury [12]. We previously reported that endoglin is expressed by EPDCs [35]. Furthermore, Bollini *et al.* (2014) showed an increased number of WT1+/endoglin+ EPDCs upon induction of MI [6]. This suggests that upregulation of endoglin in the active epicardium is part of the cardiac injury response.

Due to the important role of EPDCs following cardiac injury [34, 40], the epicardium is a tantalizing therapeutic target for cardiac regeneration. Therefore, a thorough understanding of epicardial behavior is paramount to appreciate its potential in cardiac repair. Given the deteriorated heart function following MI in *Eng*+/- mice and the pivotal role of TGFβ signaling in epicardial EMT, we investigated if endoglin contributes to the epicardial response to injury.

In this study, we analyzed the composition and the behavior of the epicardial layer at different time-points post-MI. Our data suggest that the epicardial injury response of thickening and coverage of the (diseased) myocardium with a WT1+ layer is aberrant upon endoglin heterozygosity. In the first days after MI, thickening of the epicardium in *Eng*+/- mice is less pronounced compared to wild type (wt) hearts. In contrast, at 14 days post-MI, a significantly thicker epicardial layer is observed in *Eng*+/- animals which coincides with a thinner ventricular wall. We show that these observations are not due to a difference in the epicardium at baseline and occur independently of extra-cardiac contributions from the circulation. Moreover, we found that the epicardial response can be influenced by systemic

delivery of Diprotin A, an inhibitor of CD26/dipeptidyl peptidase 4 (DPP4). Altogether, we show that endoglin is important for the post-injury response, and suggest an important role of this TGFβ co-receptor in relation to epicardial behavior.

Methods

Animals

Experiments and analyses were conducted on male and female endoglin wild type (wt) and endoglin heterozygous (*Eng*+/-) mice [3] which were maintained on a C57BL/6Jlco background (Charles River). All mouse experiments were approved by the regulatory authorities of Leiden University (The Netherlands) and were in compliance with the guidelines from Directive 2010/63/EU of the European Parliament on the protection of animals used for scientific purposes.

Induction of myocardial infarction in mice and Diprotin A treatment

Myocardial infarction (MI) was experimentally induced in male mice as described before [41]. Briefly, mice were anesthetized with isoflurane (1.5-2.5%), orally intubated and ventilated, after which the left anterior descending (LAD) coronary artery was permanently ligated by a suture. During the first 5 days post-MI, the mice were randomized and treated daily with either 100 µl distilled water (MQ) or 100 µl Diprotin A (50 µM, DipA, Bachem) via intraperitoneal injection. Mice were euthanized at 4 or 14 days after MI using carbon-dioxide.

Immunofluorescent staining

Hearts were fixed overnight at 4°C in 4% paraformaldehyde, washed with phosphate-buffered saline (PBS) followed by dehydration to xylene and embedded in paraffin. Six µm thick sections were mounted onto coated glass slides (VWR SuperFrost Plus microscope slides; Klinipath), deparaffinized and rehydrated to PBS. Antigen retrieval was performed as previously described [29]. Primary antibodies, incubated overnight at 4°C, included: anti-pSMAD1/5/9 (rabbit; dilution 1:1000 using Tyramide Signal Amplification [15]; Cell Signaling), anti-pSMAD2 (rabbit; dilution 1:200; Cell Signaling), anti-WT1 (rabbit, dilution 1:100, Abcam), anti-MAC3 (rat, dilution 1:200, BD Biosciences), anti-αSMA (rabbit, dilution 1:500, Abcam), anti-cTnI (goat, dilution 1:1000, HyTest), anti-PECAM1 (mouse, dilution 1:800, Santa Cruz) and anti-Ki67 (rabbit, dilution 1:100, Millipore). Fluorescently-labelled secondary antibodies (Invitrogen) were incubated for 1.5 hour at a 1:250 dilution. The slides were mounted with Prolong Gold-DAPI Antifade (Invitrogen) reagent.

Staining of fibrotic tissue was performed using a Picrosirius Red (PSR) collagen staining which includes deparaffinization, 1 h incubation with PSR solution, washing in acidified water and mounting with Entellan (Merck) reagent. All stainings were scanned at 40x magnification with the Pannoramic slide scanner and analyzed using CaseViewer 2.0 (3D Histech).

Morphometry
Heart sections were taken at approximately 300 µm intervals along the transverse axis of the heart. All measurements are given as average of at least three levels along the infarct area (unless otherwise stated). Infarct size was determined in PSR stained sections by calculating the percentage of infarct area of the total left ventricular area. Thickness of the ventricular wall was measured in the PSR stained sections. Measurements were taken at two separate levels along the infarct area, and given as the average of eight measurements per level.

The epicardial border zone was defined as the epicardial layer lining the 'healthy' myocardium bordering the infarct area at both sides (see also Figure 1D-E). This region was determined to be around 600 µm in length (based on [32]). The epicardial border zone included the outer epicardium (single-cell layer that surrounds the heart) and subepicardial layer (cell layer(s) between myocardium and outer epicardium), while the pericardium was excluded from analysis. Analyses of the epicardial border zone are presented as the average of both border zones.

Epicardial thickness was calculated as the average of at least four measurements per epicardial border zone (600 µm in length) or remote epicardial layer. The total cell content of the epicardial border zone was counted using DAPI staining as the total of nuclei per µm cardiac outline. Positive cells (WT1, MAC3 and Ki67) within the epicardial border zone are depicted as the percentage of total number of nuclei. Finally, pSMAD levels were quantified as the area fluorescent signal corrected for the number of nuclei within that region.

Coverage of the (injured) myocardium with a WT1+ epicardial layer was measured using the WT1 stained sections, and was quantified as the percentage WT1+ outline of the total cardiac circumference.

Culturing mouse hearts
Wt and *Eng*+/- female mouse hearts were cultured in the miniature tissue culture system [31] as previously described [25] with the following modifications. The inflow needle of the perfusion chamber was inserted in the aorta of the isolated intact heart and ligated with suture. The outflow needle was replaced with a 14 Gauge Blunt Tip Needle which allowed the medium to exit the perfusion chamber. Using a speed of 1100 µl/min, flow was introduced through the aorta directing the medium into the coronary circulation. The medium exited the heart via the right atrium and recirculated to the reservoir. After 7 days of culture the hearts were isolated and fixed overnight in 4% PFA at 4°C.

Isolation, culture and migration of human EPDCs
Adult human atrial samples (auricles) were collected as surgical waste during cardiac surgery and under general informed consent. Handling of human heart tissues was carried out according to the official guidelines of the Leiden University Medical Center and approved by the local Medical Ethics Committee. This research conforms to the Declaration of Helsinki.

EPDCs were isolated, cultured and a scratch assay was performed as previously described [35]. In short, the adult epicardium was separated from the underlying myocardium. Epicardial tissue was cut into pieces and treated with Trypsin/EDTA (Serva and USH products) at 37^0C. A single cell suspension was obtained by passing the samples through

a series of syringes. EPDCs were plated on 0.1% gelatin (Sigma) coated culture dishes in a 1:1 mixture of Dulbecco's modified Eagle's medium (DMEM-glucose low; Invitrogen) and Medium 199 (M199; Invitrogen) supplemented with 10% heat-inactivated fetal calf serum (Hi-FCS; Gibco), 100 U/ml penicillin/streptomycin (Gibco) and 10 μM SB431542 (SB; Tocris Bioscience). Scratch assays were performed with mesenchymal (spindle) EPDCs which were obtained by stimulating EPDCs with 1 ng/ml TGFβ3. Spindle EPDCs were split and grown to confluency upon which the scratch was placed. The cells were monitored for 12 hours and the percentage gap closure was measured using Matlab (version 2016a).

Statistics
Graphs are represented as mean ± SD. Samples were compared using an unpaired Student's t-test or one-way ANOVA testing for difference between multiple groups. Significance was assumed when $p<0.05$. GraphPad Prism (Version 6) was used for statistical analysis.

Results

Aberrant TGFβ signaling in *Eng*+/- epicardial layer
Since endoglin heterozygosity impairs cardiac recovery after MI and endoglin is expressed by EPDCs [35], we questioned the role of endoglin in the epicardial response post-MI. A schematic outline of the experiment together with an overview of the factors measured is presented in Figure 1A.

Given that endoglin defines the balance between the TGFβ-responsive pathways (pSMAD2/3 and pSMAD1/5) [18, 20], we performed immunofluorescence staining for pSMAD1/5/9 and pSMAD2. Both pathways are active in the epicardial layer post-MI (Figure 1B). However, we observed an increase in pSMAD1/5/9 levels in *Eng*+/- versus wt mice, while no differences were observed in pSMAD2 (Figure 1C). This indicates that endoglin heterozygosity results in altered signaling within the epicardial layer.

Epicardial thickening and activation is altered in *Eng*+/- mice at 4 days post-MI
Given the disturbed TGFβ signaling upon endoglin heterozygosity, we questioned whether this results in a difference in epicardial phenotype. First, we analyzed the epicardium and myocardium of adult non-MI mice in transverse heart sections and observed no aberrations in *Eng*+/- compared to wt animals (data not shown). Epicardial thickening upon cardiac injury has been described to occur in the entire epicardium, but is most pronounced near the infarct area [43, 44]. Therefore, we focused our analysis on the epicardium and subepicardium that lines the myocardium directly bordering the ischemic area. This region is represented as the epicardial border zone (schematically pictured in Figure 1D-E).

Four days post-injury, wt and *Eng*+/- mice showed no difference in infarct characteristics, including infarct size and infarct outline (Supplementary Figure 1A-C). However, when investigating the epicardial layer in more detail, we observed that the epicardial border zone was significantly thinner in *Eng*+/- mice (Figure 1F; wt: 22.24±3.01 *Eng*+/-: 18.77±3.47). This phenomenon was not observed at the remote area lining the right ventricle, although wt

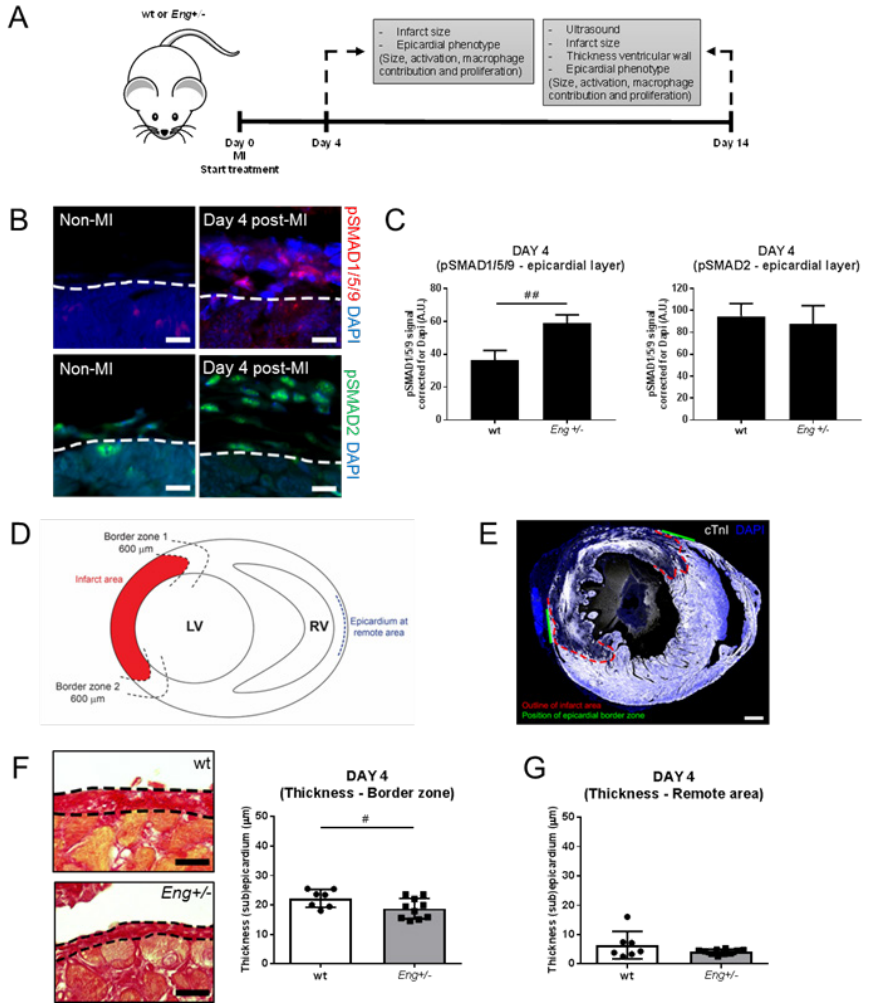

Figure 1. Aberrant TGFβ signaling and epicardial thickening in Eng+/- at 4 days post-MI. A. Overview of experiment and measured entities. Wt or Eng+/- mice were sacrificed at 4 and 14 days after the induction of MI. B. pSMAD1/5/9 and pSMAD2 are upregulated in the epicardial layer upon MI. The dashed line represents the border between myocardium and epicardium. Scale bars: 10 µm. C. Quantification of immunofluorescent stainings suggest a higher staining intensity for pSMAD1/5/9 in the epicardial layer (outlined) of Eng+/- compared to wt mice. (n = 3-4 mice for each group). Scale bars: 20 µm. D. Schematic representation of transverse section of the heart. Depicted is the infarct area (red) with at both sides a border zone. The border zone has an estimated width of 600 µm and represents 'healthy' myocardium lining the infarct area. The remote area is at the right ventricle, opposite to the infarct. E. Example of transverse section of the infarcted heart. The red line represents the border between infarcted and 'healthy' myocardium. The green lines show the position of the investigated epicardial layer at both border zones with a length of 600 µm. Scale bar: 500 µm. F. In PSR stainings, the outer collagen layer at the border zone (outlined; scale bars: 20 µm) is thinner in Eng+/- mice (n = 7-10 mice for each group). G. The thickness of the epicardial layer at a remote area is equal between Eng+/- and wt hearts (n = 7-10 mice for each group). Data information: #: p<0.05 and # #: p<0.01

mice displayed a larger variation in thickness (Figure 1G).

The thinner epicardial border zone after induction of MI can be explained by the presence of fewer cells within this region in *Eng*+/- compared to wt mice (Figure 2A-B). Interestingly, not only the border zone, but the entire epicardial layer contains less cells in *Eng*+/- hearts (Figure 2C). A difference in cell number within the epicardial region could be the result of a defect in cell proliferation. Therefore, we determined the number of cycling cells by performing a Ki67 staining (Figure 2D). However, no difference in the percentage of Ki67+ cells within the epicardial border zone in *Eng*+/- compared to wt mice was observed (Figure 2E).

The expression of WT1 in the epicardium is considered to be one of the first steps in epicardial activation post-injury [14]. Although the *Eng*+/- epicardial border zone contains a reduced number of total cells, we observed a higher percentage of WT1+ cells within this region compared to the wt border zone (Figure 2F-G). Since epicardial activation occurs organ-wide, including the remote area, we quantified the presence of WT1+ cells within the entire epicardial layer. Consistent with the border zone, the percentage of WT1+ cells throughout the epicardial layer was significantly higher in *Eng*+/- mice compared to wt animals (Figure 2H). This difference in WT1 is not related to the infarct size, indicating that it does not result from a difference in cardiac damage (data not shown). In addition, we observed no difference in the expression of the epicardial activation markers WT1 and Transcription factor 21 (TCF21; [1, 8]) in non-infarcted wt and *Eng*+/- hearts (data not shown). This suggests that the increased percentage of WT1+ cells in *Eng*+/- mice at 4 days post-MI is not caused by a difference in epicardial activity at baseline.

In summary, the thinner epicardial layer in *Eng*+/- mice at 4 days post-MI is the result of a lower number of cells within the (sub)epicardial space. Our data suggest no difference in proliferation (at 4 days post-MI) and endoglin heterozygosity does not lead to an aberrant epicardial and myocardial phenotype at baseline. This suggests that the difference in the epicardium between wt and *Eng*+/- mice is directly caused by the induced injury and its related processes. Furthermore, a higher percentage of WT1+ cells indicates a difference in composition and activation of the *Eng*+/- epicardial layer.

Epicardial phenotype in *Eng*+/- mice is independent of extra-cardiac cell contributions

We further investigated the contribution of circulating cells to the phenotype of the (sub) epicardium in *Eng*+/- and wt mice. The subepicardial space is known to harbor immune cells [16, 21]. Zhou *et al.* reported infiltration of monocytes into the epicardial layer following MI [44]. We previously observed that *Eng*+/- mononuclear cells have a reduced ability to migrate towards the infarct area [26, 38]. Therefore, the presence of immune-reactive cells, as an extra-cardiac derived cell source, could contribute to a difference in total epicardial cell count. Macrophages are the major cell type invading the heart upon MI [27]. We analyzed the number of macrophages in the epicardial border zone by staining for MAC3 (LAMP2/CD107b). There is no overlap between WT1 and MAC3 expression, indicating that the WT1+ cells are not macrophages (Figure 3A). In addition, at 4 days post-MI we observed no difference in the percentage of macrophages within the epicardial border zone (Figure 3B) suggesting that the presence of macrophages is not the cause of a decreased presence of (sub) epicardial cells within the *Eng*+/- epicardial border zone compared to wt.

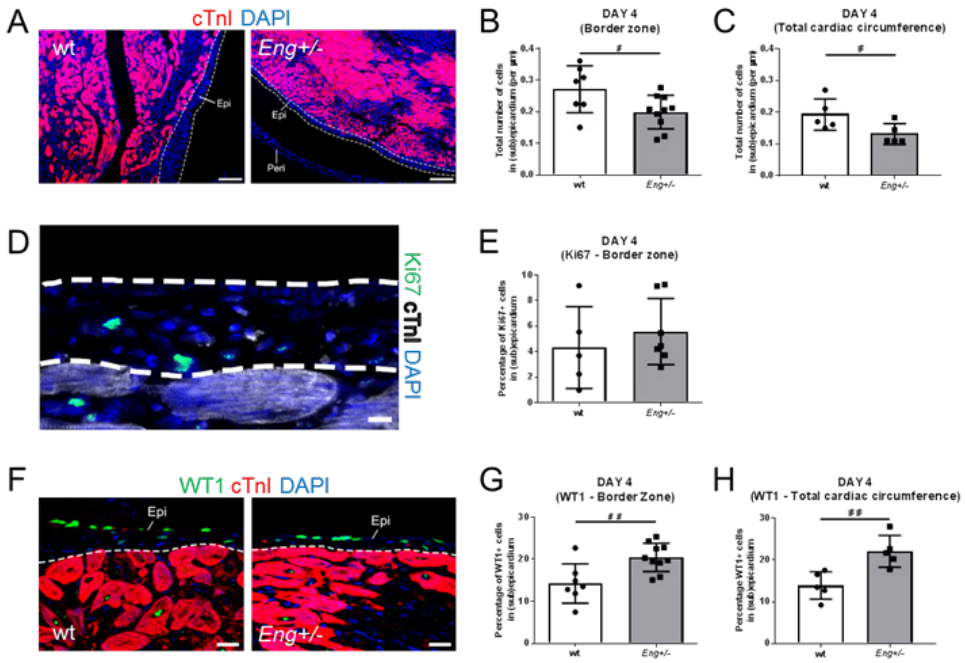

Figure 2. Altered composition of the Eng+/- epicardial layer. A. Cardiac troponin I (cTnI)/DAPI immunofluorescence stainings show the wt and Eng+/- epicardial border zone which are located in between the dashed lines. Epi: (sub)epicardium, Peri: pericardium. Scale bar: 100 µm. B,C. The number of cells was quantified for the epicardial layer lining B. the border zone (n = 7-10 mice for each group) and C. total cardiac circumference (n = 5 mice for each group). D,E The percentage of Ki67+ cells within the epicardial border zone is equal between Eng+/- and wt mice (n = 5-7 mice for each group). Scale bar: 10 µm. F-H. WT1 immunofluorescence staining of the wt and Eng+/- epicardial border zone. In F. the dashed line represents the border between myocardium and (sub)epicardium. Scale bar: 20 µm. Epi: (sub)epicardium, Peri: pericardium. In Eng+/- mice, a higher percentage of epicardial cells is positive for WT1 compared to wt animals in both G. the epicardial border zone (n = 7-10 mice for each group) and H. the entire epicardial layer (n = 5 mice for each group). Data information: #: p<0.05 and # #: p<0.01

To investigate the extra-cardiac cell contribution in more detail, we analyzed thickening of the epicardium in the absence of circulating cells. We cultured wt and *Eng+/-* hearts *ex vivo* in a continuous flow of culture medium using a novel miniature tissue culture system [25, 31]. As a result of the *ex vivo* culture conditions, the epicardial layer is activated and responds by becoming thicker. Interestingly, in *Eng+/-* hearts the thickening of the epicardial layer was significantly less pronounced as compared to wt (Figure 3C-D). This indicates that a thinner epicardial layer in *Eng+/-* mice occurs independently of extra-cardiac cell contributions from the circulation.

Coverage of the infarcted heart with a WT1+ epicardial layer is altered in *Eng+/-* mice at 4 days post-MI

The organ-wide re-expression of WT1 in the epicardial layer is a spatio-temporal dynamic process, peaking between day 1 and 5 post-MI [43, 44]. Interestingly, at day 4 post-MI, a

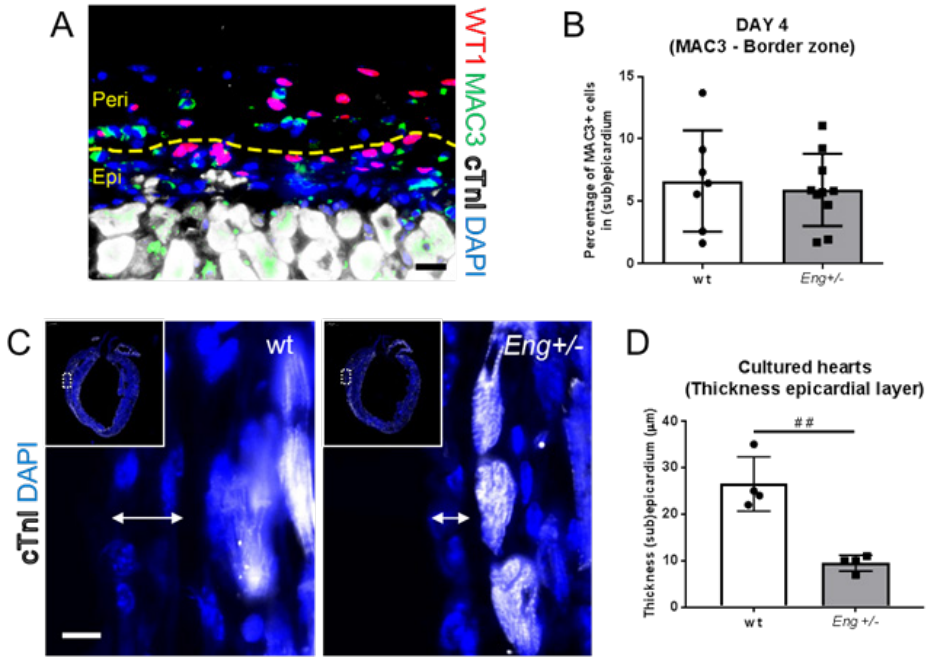

Figure 3. Epicardial phenotype in Eng+/- mice is independent of extra-cardiac cell contributions. A. Immunofluorescence staining shows that there is no overlap between WT1+ and MAC3+ cells in the epicardial border zone. The dashed line represents the border between (sub)epicardium and pericardium, Epi: (sub)epicardium, Peri: pericardium. Scale bar: 10 µm. B. Quantification of MAC3+ cells in the (sub)epicardium. No difference was observed in the percentage of MAC3+ cells within the epicardial border zone between wt or Eng+/- hearts (n = 7-10 mice for each group). C. Longitudinal section of a wt and Eng+/- cultured heart highlighting the epicardial layer (white arrows). cTnI=white, DAPI=blue. Scale bar: 10 µm. D. The thickness of the epicardial layer as measured in sections of cultured hearts of wt and Eng+/- mice (n = 4 mice for each group). Data information: # #: p<0.01

larger part of the cardiac circumference was covered by a WT1+ epicardial layer in *Eng*+/- compared to wt mice (Figure 4A-B). This difference in WT1 coverage is not related to the infarct size (data not shown). We questioned whether this altered coverage could result from a difference in migration rate. Therefore we modulated endoglin expression in EPDCs and performed an *in vitro* scratch assay. Strikingly, upon endoglin knockdown, epicardial cells migrate significantly faster (Figure 4C). Overall, these data suggest altered epicardial behavior upon endoglin heterozygosity, including increased migration and coverage of the infarcted heart with a WT1+ epicardial layer.

Thicker epicardial layer in *Eng*+/- mice at day 14 post-MI

In contrast to day 4, at 14 days post-MI we observed a significantly thicker epicardial layer at both the border zone (Figure 5A) and the remote area (Figure 5B) in *Eng*+/- compared to wt mice. In addition, the *Eng*+/- epicardial border zone contained more cells (Figure 5C). Interestingly, wt animals displayed a decrease in the size of the epicardial border zone from day 4 to day 14 post-MI (from ±23 µm to ±17 µm). In contrast, in *Eng*+/- mice the thickness

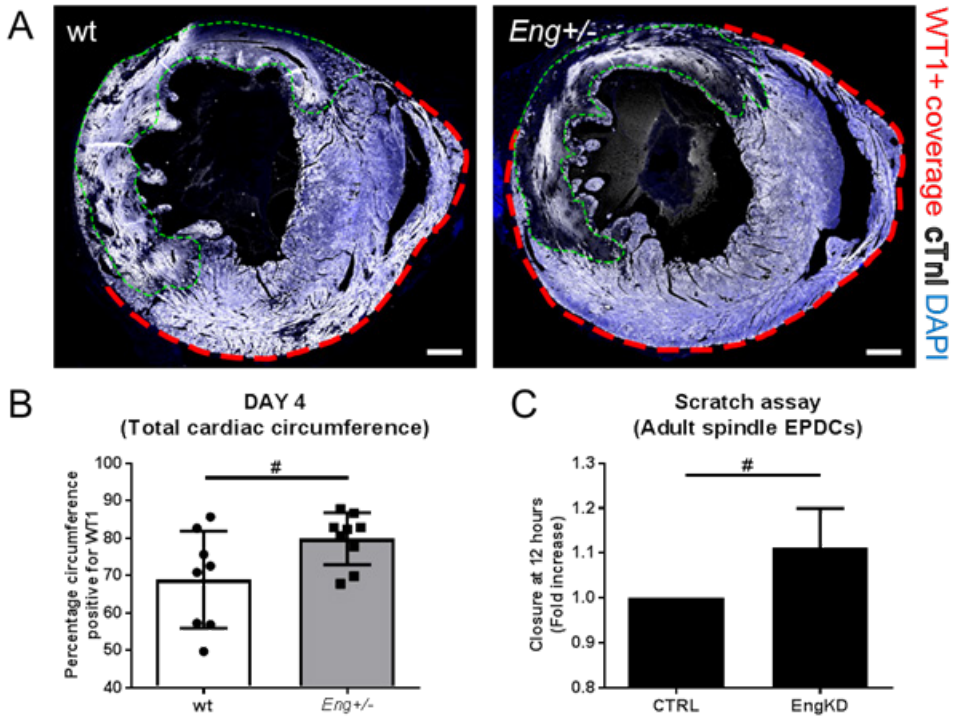

Figure 4. Coverage of the infarcted heart with a WT1+ epicardial layer is altered in Eng+/- mice at 4 days post-MI. A. The pattern of activation of the epicardial layer at day 4 is represented by the percentage of cardiac circumference covered by a WT1+ epicardial layer. The infarct is outlined in green and the epicardial layer positive for WT1 is marked by a red dotted line. Scale bars: 500 µm. B. In Eng+/- mice, a higher percentage of the circumference is positive for WT1 (n = 8-9 mice for each group). C. Upon endoglin knockdown (KD) human adult EPDCs migrate faster in a scratch assay (n = 5 measurements). Data information: #: p<0.05

of the epicardial layer continues to increase over time (from ±19 µm to ±26 µm) suggesting a delay in epicardial thickening upon MI.

As a potential underlying cause of a thicker epicardial layer in *Eng*+/- mice, differences in the degree of activation (WT1 expression) and proliferation were studied. At day 14 post-MI, the entire cardiac circumference was covered with a WT1+ epicardial layer with no difference between *Eng*+/- and wt mice (data not shown). Moreover, we observed no difference in the presence of WT1+ (Figure 5D) or Ki67+ (Figure 5E) cells within the epicardial border zone. This suggests that epicardial activation and cell proliferation are not aberrant at 14 days post-MI upon endoglin heterozygosity.

It was previously shown that the clearance of inflammatory cells is impaired in *Eng*+/- mice [37]. Therefore we analyzed the presence of MAC3+ cells within the epicardial region. Compared to day 4, the total number of MAC3+ cells in the epicardial border zone in both groups is low (from ±6 percent at day 4 to ±2 percent at day 14). Furthermore, the percentage of MAC3+ cells within the epicardial border zone was equal between wt and *Eng*+/- animals (Figure 5F), showing that there was no defect in clearance of macrophages from the epicardial border zone.

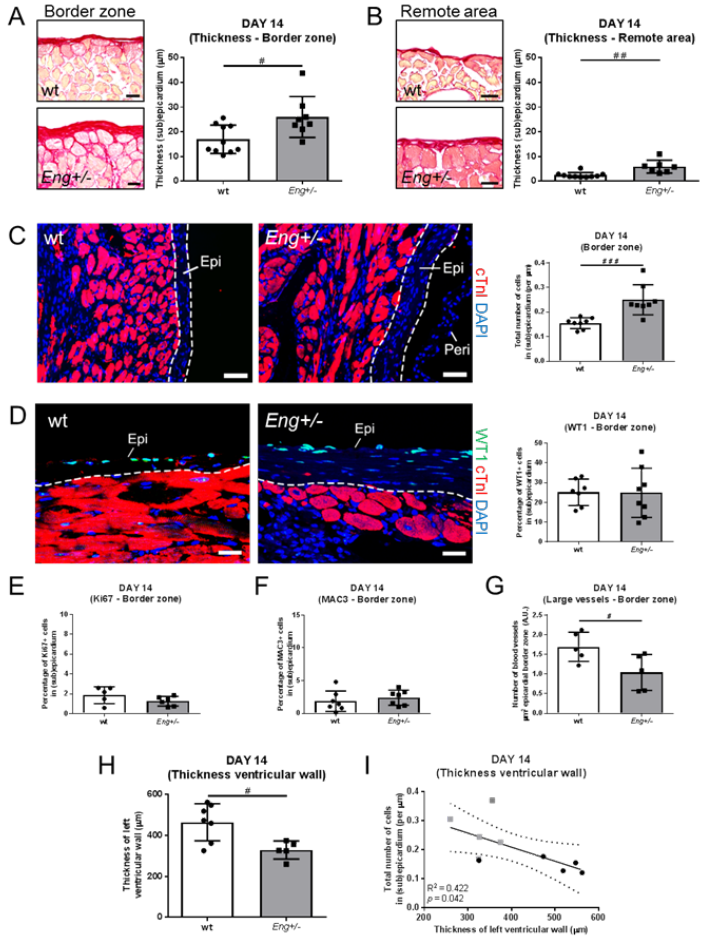

Figure 5. Delayed epicardial thickening in Eng+/- mice at day 14 post-MI is related to thinner ventricular wall. A-C. The collagen layer (representing the epicardial layer) is thicker in Eng+/- animals (Scale bar: 20µm) both at A. the border zone and B. a remote region. C. The epicardial border zone of Eng+/- mice contains more cells. The dashed lines outline the epicardial layer (n = 7-10 mice for each group). Scale bar: 50µm. D. The percentage of WT1 positive cells within the epicardial border zone is equal between wt and Eng+/- mice. The dashed lines indicate the boundary between myocardium and (sub)epicardium (n = 7-8 mice for each group). Scale bar: 20µm. E,F. The percentage of E. Ki67+ (n = 5-6 mice for each group) and F. MAC3+ cells is equal between wt and Eng+/- mice in the epicardial border zone (n = 7 mice for each group). G. Number of blood vessels per µm2 epicardial border zone (A.U.) at day 14 post-MI. Eng+/- mice have a lower density of large blood vessels compared to wt (n = 5 mice for each group). H. Ventricular wall thickness (µm). At day 14 post-MI, the left ventricular wall is thinner in Eng+/- compared to wt animals (n = 5-7 mice for each group). I. Correlation of the total number of cells in (sub) epicardium (per µm) to the thickness of the left ventricular wall (µm). A negative correlation was observed between the total number of cells within the epicardial border zone and the thickness of the left ventricular wall. Eng+/- mice are depicted in grey/square data points (n = 5 mice for each group). Data information: Epi: (sub)epicardium, Peri: pericardium and #: p<0.05, # #: p<0.01 and # # #: p<0.005

Since the epicardium develops in close relation to the coronary vasculature [28] and endoglin plays an important role during angiogenesis, we quantified the blood vessel content (large blood vessels and capillaries) of the epicardial border zone (Supplementary Figure 2). We observed a lower density of large (non-capillary) blood vessels in *Eng*+/- mice (Figure 5G), suggesting that the thicker epicardial border zone is not due to a difference in the number of vessels. Therefore, it appears that the thicker *Eng*+/- epicardial border zone at 14 days post-MI is caused by an increase in (sub)epicardial cells. In *Eng*+/- mice, myocardial infarction results in greater deterioration of heart function compared to wt animals [26]. At 14 days post-infarct we detected a significant thinner left ventricular wall in *Eng*+/- mice (Figure 5H). Therefore, we investigated whether a greater cardiac damage is associated with a thicker epicardial border zone at 14 days post-MI. We observed no correlation between the number of cells within the epicardial border zone and the infarct size of wt and *Eng*+/- mice (Supplementary Figure 3). Furthermore, the size of the epicardial border zone was not correlated to the percentage of ejection fraction (data not shown). Interestingly, however, the total number of cells within the epicardial border zone is negatively correlated with the thickness of the left ventricular wall (Figure 5I).

Our data strongly suggest that thickening of the (sub)epicardial layer is dysregulated in *Eng*+/- mice and the size of this layer correlates to the thickness of the left ventricular wall.

DipA treatment significantly alters the epicardial post-MI response

We questioned whether we can reduce the epicardial size (thickness and number of cells) of *Eng*+/- hearts at day 14 post-MI to wt levels, given its correlation with a thinner left ventricular wall. The highly conserved SDF1/C-X-C motif chemokine receptor 4 (CXCR4) signaling axis plays an essential role in the epicardial/myocardial crosstalk during cardiac healing [22]. In addition, EPDCs express CXCR4 (data not shown) and TGFβ signaling influences the SDF1/CXCR4 axis [2, 36, 38].

Wt and *Eng*+/- mice were treated with DipA or MQ for the first 5 days following induction of MI (Figure 6A). DipA is a selective inhibitor of CD26/DPP4 and thereby a positive modulator of SDF1-CXCR4 interaction. DipA treatment has been shown to increase migration and homing of cells [10]. Indeed, at 4 days post-MI, DipA treatment significantly increased the number of MAC3+ cells localized to the epicardial border zone of *Eng*+/- animals (Supplementary Figure 4A). This suggests that DipA treatment was effective, as it resulted in increased homing of immune-reactive cells towards the site of injury.

We next investigated the long-term (14 days post-MI) effect of DipA administration. Strikingly, after DipA treatment the thickness of the epicardial border zone in *Eng*+/- mice is reduced to wt levels (Figure 6B). The reduction in epicardial size could be explained by a decrease in the total number of cells and was related to a significantly thicker ventricular wall in DipA treated *Eng*+/- animals (grey bars in Figure 6C-E). In contrast, in wt mice we observed a significant increase in the number of cells within the epicardial border zone and a trend towards a decrease in left ventricular wall thickness upon treatment (white bars in Figure 6C-E). This change in epicardial size was not due to a difference in macrophage percentage, since we observed no significant changes in the presence of MAC3+ cells within the epicardial border zone (Supplementary Figure 4B). Altogether our data demonstrate that systemic administration of DipA influences the epicardial phenotype. More importantly, they suggest that, for *Eng*+/- animals, DipA treatment during the first week following MI results in restoration of epicardial thickness to wt levels and limited left ventricular wall thinning.

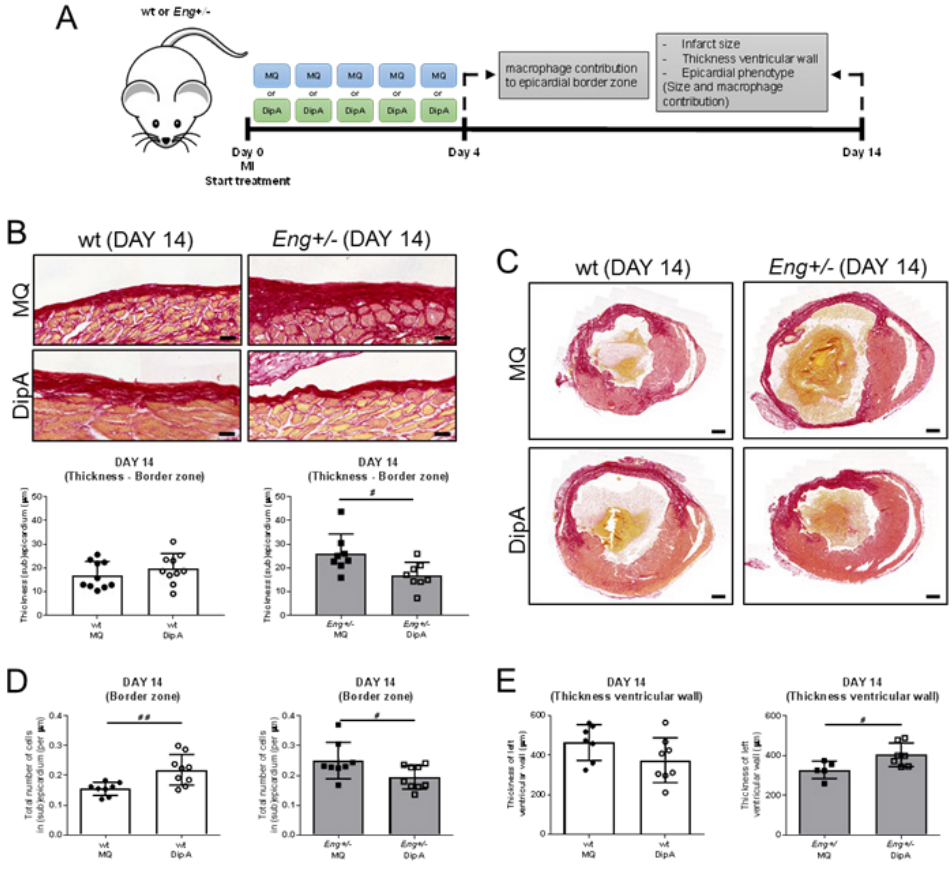

Figure 6. DipA treatment significantly alters the epicardial post-MI response at 14 days post-MI. A. Overview of experiment and measured entities. Wt or Eng+/- mice were given Diprotin A (DipA) or control (MQ) treatment and sacrificed at day 4 and day 14 after the induction of MI. B. PSR stainings of the wt and Eng+/- epicardial border zone (Scale bars: 20 µm). DipA administration significantly decreases the thickness of the epicardium in Eng+/- mice while no change was observed in wt animals (n = 8-10 mice for each group). C. PSR stainings of wt and Eng+/- transverse heart sections, MQ or DipA treated, showing the thickness of the left ventricular wall (Scale bar: 500 µm). D. DipA treatment significantly increases and decreases the total number of epicardial cells at border zone for wt and Eng+/- animals, respectively (n = 8-9 mice for each group). E. DipA treatment significantly increases the thickness of the left ventricular wall in Eng+/- animals (n = 5-8 mice for each group). Data information: #: p<0.05 # #: p<0.01

Discussion

The mechanisms underlying the behavior of the epicardial layer following MI are not fully understood which makes it difficult to use this layer as a source for repair of cardiac injury. Using *Eng*+/- mice, our data indicate an important role for endoglin in the epicardial MI-response. Higher pSMAD1 levels in the *Eng*+/- epicardial layer suggest a misbalance within the TGFβ signaling pathway. We observed aberrant epicardial thickening in *Eng*+/- hearts which appears to occur independently of extra-cardiac cell contributions from the circulation. At day 4 post-MI, the *Eng*+/- epicardial layer harbors a higher percentage of WT1+ cells suggesting increased activation of this layer. In addition, the correlation between the thickness of the epicardial layer and ventricular wall strengthens the importance of studying the epicardium as a myocardial support mechanism. Moreover, in *Eng*+/- mice the thickness of the epicardial border zone and ventricular wall were reversed to wt levels upon systemic administration of DipA.

Besides angiogenesis, endoglin appears to be important for a fully functional immune system [12] and a change in the immune response may be the underlying cause of a difference in epicardial phenotype. *Eng*+/- mononuclear cells are impaired in their homing capacity to the infarcted heart [26, 38] and persistent inflammation was observed in *Eng*+/- mice following injury [37]. As a consequence, a thinner epicardial layer in *Eng*+/- animals at day 4 could have been the result of a potential delayed immune response, while a thicker layer at day 14 may be due to persistent inflammation. Therefore, we cultured wt and *Eng*+/- hearts *ex vivo*, without the presence of circulating immune cells. Interestingly, also in culture we observed a thinner epicardial layer in *Eng*+/- compared to wt suggesting an intrinsic defect occurring independently of extra-cardiac cell contributions. However, we cannot exclude the contribution of resident immune cells. From another point of view, Huang and colleagues showed that inhibition of epicardial activation results in reduced number of immune cells in the infarcted area [21]. This observation suggests that the defects in MI-induced inflammation in *Eng*+/- mice may also be caused by aberrant epicardial behavior. However, future studies will be required to dissect a potential cross-talk between the epicardium and immune-system in more detail.

After MI, the epicardium lining the infarct area is lost. Cells from the epicardial border zones proliferate and gradually close the (epicardial) gap, ultimately covering the infarct surface with a WT1+ epicardial layer [43]. At 4 days following MI, *Eng*+/- hearts had a higher percentage of their cardiac circumference covered with a WT1+ layer which may be related to an increased migration rate of EPDCs upon partial loss of endoglin. Increased migration of EPDCs may result a faster closure of the epicardial gap in *Eng*+/- mice and as a consequence a higher coverage of the infarcted heart with a WT1+ epicardial layer.

A higher percentage of WT1+ cells results in an altered composition of the *Eng*+/- epicardial layer compared to wt animals which may cause paracrine changes in the cardiac environment. The transcription factor WT1 is, besides a marker for epicardial activation, an important regulator of epicardial EMT [5, 14, 17, 33, 42]. Upon activation, epicardial cells undergo EMT and form the subepicardium. When EPDCs go through EMT, they lose their nuclear expression of WT1 [5]. A higher percentage of WT1+ cells within the epicardial layer may indicate increased activation or affected transition through EMT causing *Eng*+/- EPDCs to remain in a WT1+ stadium for an extended period of time. Alternatively, potential increased migration of WT1-EPDCs into the underlying myocardium may result in a thinner epicardial layer and as a consequence a higher proportion of WT1+ cells within this layer. Which of these mechanisms underlie the altered size and composition of the *Eng*+/- epicardial layer

shortly after MI is an important aspect of future research.

Partial loss of endoglin can have both a detrimental and beneficial effect on heart function which appears to be dependent on the underlying cause of the disease [23, 26]. In a mouse model of pressure-overload induced heart failure, endoglin deficiency has been shown to preserve left ventricular function resulting in increased survival [23]. Our data suggest that there is a correlation between the number of cells within the (sub)epicardial layer and thickness of the left ventricular wall. A defect in the epicardial response following MI has been reported to result in ventricular dilatation and reduced cardiac performance [13]. Therefore, an increase in epicardial size may be the underlying cause of a thinner ventricular wall. However, a thicker epicardial layer may also be a protective mechanism contributing to reducing heart failure and cardiac rupture. Whether the observed changes in epicardial behavior upon partial loss of endoglin are beneficial for cardiac repair remains subject to future studies.

The epicardium plays an important role as a myocardial support mechanism. The correlation between the size of the epicardial layer and left ventricular wall may indeed suggest a dialog with the underlying myocardium. The SDF1/CXCR4 axis has been proposed to be an important endogenous pathway involved in epicardial-myocardial crosstalk [22]. Upon MI, SDF1 is upregulated in the myocardium [4] and EPDCs are able to migrate towards the SDF1 chemokine [39]. Our data suggest that enhancing this pathway, via DipA treatment, results in fewer epicardial cells within the epicardial region. This might point towards, besides a potential alteration in the extra-cardiac cell contribution, an increased homing of EPDCs towards the underlying diseased myocardium. DipA treatment could increase the migration ability of EPDCs in the direction of myocardial SDF1 via the inhibition of its catalytic enzyme, DPP4. In this context, it is interesting to note that human *Eng+/-* mononuclear cells have a misbalanced SDF1/CXCR4 axis resulting in reduced homing towards a SDF1 gradient. In addition, DipA pre-treatment of these human *Eng+/-* mononuclear cells enhanced their homing capacity towards to injured myocardium upon injection into the tail vein [38].

The epicardium plays an important role following cardiac injury. This layer has been proposed to serve as an endogenous source of cardiovascular cell types and/or support the myocardium via paracrine signaling, both during the early phase following injury as during scar modulation [40]. In conclusion, our data give an insight in epicardial behavior following injury and suggest that endoglin is an important player in this context. These new insights may help in exploiting the epicardium as a therapeutic target for cardiac repair and regeneration.

Acknowledgements

We thank the remaining members of our group for valuable discussions and W.C.R. Sloos, J.C.A.G. Wiegant and A.M.A van der Laan for technical assistance. We thank Prof. Dr. P. ten Dijke (Department of Molecular Cell Biology, LUMC, Leiden, the Netherlands), and J.C. Peterson and Prof. Dr. M.C. de Ruiter (Department of Anatomy and Embryology, LUMC, Leiden, the Netherlands) for providing antibodies. We are grateful to the department of Cardiothoracic Surgery (LUMC, Leiden, the Netherlands) for collecting and providing human adult heart tissue.

Conflict of interest
The authors declare that they have no conflict of interest.

Funding
This work was supported by the Netherlands Institute for Regenerative Medicine (NIRM1.7), the Dutch Heart Foundation (30710), the ZonMw-TAS program (116002016), the Netherlands Organization for Scientific Research (NWO) VENI (016.146.079) (AM Smits) and a LUMC Research fellowship (AM Smits).

References
1. Acharya A, Baek ST, Huang G, Eskiocak B, Goetsch S, Sung CY, Banfi S, Sauer MF, Olsen GS, Duffield JS, Olson EN, Tallquist MD (2012) The bHLH transcription factor Tcf21 is required for lineage-specific EMT of cardiac fibroblast progenitors. Development 139:2139–2149. doi: 10.1242/dev.079970

2. Ao M, Franco OE, Park D, Raman D, Williams K, Hayward SW (2007) Cross-talk between paracrine-acting cytokine and chemokine pathways promotes malignancy in benign human prostatic epithelium. Cancer Res 67:4244–4253. doi: 10.1158/0008-5472.CAN-06-3946

3. Arthur HM, Ure J, Smith a J, Renforth G, Wilson DI, Torsney E, Charlton R, Parums D V, Jowett T, Marchuk D a, Burn J, Diamond a G (2000) Endoglin, an ancillary TGFbeta receptor, is required for extraembryonic angiogenesis and plays a key role in heart development. Dev Biol 217:42–53. doi: 10.1006/dbio.1999.9534

4. Askari AT, Unzek S, Popovic ZB, Goldman CK, Forudi F, Kiedrowski M, Rovner A, Ellis SG, Thomas JD, DiCorleto PE, Topol EJ, Penn MS (2003) Effect of stromal-cell-derived factor 1 on stem-cell homing and tissue regeneration in ischaemic cardiomyopathy. Lancet 362:697–703. doi: 10.1016/S0140-6736(03)14232-8

5. Bax NAM, Van Oorschot AAM, Maas S, Braun J, Van Tuyn J, De Vries AAF, Gittenberger-De Groot AC, Goumans MJ (2011) In vitro epithelial-to-mesenchymal transformation in human adult epicardial cells is regulated by TGFβ-signaling and WT1. Basic Res Cardiol 106:829–847. doi: 10.1007/s00395-011-0181-0

6. Bollini S, Vieira JMN, Howard S, Dubè KN, Balmer GM, Smart N, Riley PR (2014) Re-activated adult epicardial progenitor cells are a heterogeneous population molecularly distinct from their embryonic counterparts. Stem Cells Dev 23:1719–30. doi: 10.1089/scd.2014.0019

7. Bourdeau A, Dumont DJ, Letarte M (1999) A murine model of hereditary hemorrhagic telangiectasia. J Clin Invest 104:1343–51. doi: 10.1172/JCI8088

8. Braitsch CM, Combs MD, Quaggin SE, Yutzey KE (2012) Pod1/Tcf21 is regulated by retinoic acid signaling and inhibits differentiation of epicardium-derived cells into smooth muscle in the developing heart. Dev Biol 368:345–357. doi: 10.1016/j.ydbio.2012.06.002

9. Carmona R, Guadix JA, Cano E, Ruiz-Villalba A, Portillo-Sánchez V, Pérez-Pomares JM, Muñoz-Chápuli R (2010) The embryonic epicardium: An essential element of cardiac development. J Cell Mol Med 14:2066–2072. doi: 10.1111/j.1582-4934.2010.01088.x

10. Christopherson KW, Hangoc G, Mantel CR, Broxmeyer HE (2004) Modulation of hematopoietic stem cell homing and engraftment by CD26. Science (80-) 305:1000–1003. doi: 10.1126/science.1097071

11. ten Dijke P, Goumans M-J, Pardali E (2008) Endoglin in angiogenesis and vascular diseases. Angiogenesis 11:79–89. doi: 10.1007/s10456-008-9101-9

12. Dingenouts CKE, Goumans MJ, Bakker W (2015) Mononuclear cells and vascular repair in HHT. Front Genet. doi: 10.3389/fgene.2015.00114

13. Duan J, Gherghe C, Liu D, Hamlett E, Srikantha L, Rodgers L, Regan JN, Rojas M, Willis M, Leask A, Majesky M, Deb A (2012) Wnt1/βcatenin injury response activates the epicardium and cardiac fibroblasts to promote cardiac repair. EMBO J 31:429–42. doi: 10.1038/emboj.2011.418

14. Duim SN, Goumans M-J, Kruithof BPT (2016) WT1 in Cardiac Development and Disease. Wilms Tumor. doi: 10.15586/codon.wt.2016.ch13

15. Duim SN, Kurakula K, Goumans MJ, Kruithof BPT (2015) Cardiac endothelial cells express Wilms' tumor-1. Wt1 expression in the developing, adult and infarcted heart. J Mol Cell Cardiol 81:127–135. doi: 10.1016/j.yjmcc.2015.02.007

16. Gherghiceanu M, Popescu LM (2009) Human epicardium: Ultrastructural ancestry of mesothelium and mesenchymal cells. J Cell Mol Med 13:2949–2951. doi: 10.1111/j.1582-4934.2009.00869.x

17. von Gise A, Zhou B, Honor LB, Ma Q, Petryk A, Pu WT (2011) WT1 regulates epicardial epithelial to mesenchymal transition through beta-catenin and retinoic acid signaling pathways. Dev Biol 356:421–431. doi: S0012-1606(11)00983-3 [pii]10.1016/j.ydbio.2011.05.668

18. Goumans M-J, Dijke P ten (2017) TGF-β Signaling in Control of Cardiovascular Function. Cold Spring Harb Perspect Biol. doi: 10.1101/cshperspect.a022210

19. Goumans M-J, Liu Z, ten Dijke P (2009) TGF-beta signaling in vascular biology and dysfunction. Cell Res 19:116–27. doi: 10.1038/cr.2008.326

20. Goumans M-J, Zwijsen A, Dijke P ten, Bailly S (2017) Bone Morphogenetic Proteins in Vascular Homeostasis and Disease. Cold Spring Harb Perspect Biol. doi: 10.1101/cshperspect.a031989

21. Huang GN, Thatcher JE, McAnally J, Kong Y, Qi X, Tan W, DiMaio JM, Amatruda JF, Gerard RD, Hill JA, Bassel-Duby R, Olson EN (2012) C/EBP Transcription Factors Mediate Epicardial Activation During Heart Development and Injury. Science 338:1599–1603. doi: 10.1126/science.1229765

22. Itou J, Oishi I, Kawakami H, Glass TJ, Richter J, Johnson A, Lund TC, Kawakami Y (2012) Migration of cardiomyocytes is essential for heart regeneration in zebrafish. Development 139:4133–42. doi: 10.1242/dev.079756

23. Kapur NK, Wilson S, Yunis AA, Qiao X, MacKey E, Paruchuri V, Baker C, Aronovitz MJ, Karumanchi SA, Letarte M, Kass DA, Mendelsohn ME, Karas RH (2012) Reduced endoglin activity limits cardiac fibrosis and improves survival in heart failure. Circulation 125:2728–2738. doi: 10.1161/CIRCULATIONAHA.111.080002

24. Kennedy-Lydon T, Rosenthal N (2015) Cardiac regeneration: epicardial mediated repair. Proc R Soc B Biol Sci 282:20152147. doi: 10.1098/rspb.2015.2147

25. Kruithof B, Lieber S, Kruithof-de Julio M, Gaussin V, Goumans M (2015) Culturing Mouse

Cardiac Valves in the Miniature Tissue Culture System. J Vis Exp. doi: 10.3791/52750

26. Van Laake LW, Van Den Driesche S, Post S, Feijen A, Jansen MA, Driessens MH, Mager JJ, Snijder RJ, Westermann CJJ, Doevendans PA, Van Echteld CJA, Ten Dijke P, Arthur HM, Goumans MJ, Lebrin F, Mummery CL (2006) Endoglin has a crucial role in blood cell-mediated vascular repair. Circulation 114:2288–2297. doi: 10.1161/CIRCULATIONAHA.106.639161

27. Lambert JM, Lopez EF, Lindsey ML (2008) Macrophage roles following myocardial infarction. Int J Cardiol 130:147–158. doi: 10.1016/j.ijcard.2008.04.059

28. Lavine KJ, Ornitz DM (2008) Fibroblast growth factors and Hedgehogs: at the heart of the epicardial signaling center. Trends Genet 24:33–40. doi: 10.1016/j.tig.2007.10.007

29. Leung HW, Moerkamp AT, Padmanabhan J, Ng S-W, Goumans M-J, Choo A (2015) mAb C19 targets a novel surface marker for the isolation of human cardiac progenitor cells from human heart tissue and differentiated hESCs. J Mol Cell Cardiol 82:228–37. doi: 10.1016/j.yjmcc.2015.02.016

30. Li DY, Sorensen LK, Brooke BS, Urness LD, Davis EC, Taylor DG, Boak BB, Wendel DP (1999) Defective angiogenesis in mice lacking endoglin. Science 284:1534–1537. doi: 10.1126/science.284.5419.1534

31. Lieber SC, Kruithof BPT, Aubry N, Vatner SF, Gaussin V (2010) Design of a miniature tissue culture system to culture mouse heart valves. Ann Biomed Eng 38:674–82. doi: 10.1007/s10439-010-9922-8

32. Loennechen JP, Støylen A, Beisvag V, Wisløff U, Ellingsen O (2001) Regional expression of endothelin-1, ANP, IGF-1, and LV wall stress in the infarcted rat heart. Am J Physiol Heart Circ Physiol 280:H2902-10. doi: 0363-6135/01

33. Martínez-Estrada OM, Lettice LA, Essafi A, Guadix JA, Slight J, Velecela V, Hall E, Reichmann J, Devenney PS, Hohenstein P, Hosen N, Hill RE, Muñoz-Chapuli R, Hastie ND (2010) Wt1 is required for cardiovascular progenitor cell formation through transcriptional control of Snail and E-cadherin. Nat Genet 42:89–93. doi: 10.1038/ng.494

34. Masters M, Riley PR (2014) The epicardium signals the way towards heart regeneration. Stem Cell Res 13:683–692. doi: 10.1016/j.scr.2014.04.007

35. Moerkamp AT, Lodder K, Herwaarden T van, Dronkers E, Dingenouts CKE, Tengström FC, Brakel TJ van, Goumans M-J, Smits AM (2016) Human fetal and adult epicardial-derived cells: a novel model to study their activation. Stem Cell Res Ther. doi: 10.1186/s13287-016-0434-9

36. Nakamura T, Shinriki S, Jono H, Guo J, Ueda M, Hayashi M, Yamashita S, Zijlstra A, Nakayama H, Hiraki A, Shinohara M, Ando Y (2015) Intrinsic TGF-β2-triggered SDF-1-CXCR4 signaling axis is crucial for drug resistance and a slow-cycling state in bone marrow-disseminated tumor cells. Oncotarget 6:1008–1019. doi: 10.18632/oncotarget.2826

37. Peter MR, Jerkic M, Sotov V, Douda DN, Ardelean DS, Ghamami N, Lakschevitz F, Khan MA, Robertson SJ, Glogauer M, Philpott DJ, Palaniyar N, Letarte M (2014) Impaired resolution of inflammation in the Endoglin heterozygous mouse model of chronic colitis. Mediators Inflamm. doi: 10.1155/2014/767185

38. Post S, Smits AM, Van Den Broek AJ, Sluijter JPG, Hoefer IE, Janssen BJ, Snijder RJ, Mager JJ, Pasterkamp G, Mummery CL, Doevendans PA, Goumans MJ (2010) Impaired recruitment of HHT-1 mononuclear cells to the ischaemic heart is due to an altered CXCR4/CD26 balance. Cardiovasc Res 85:494–502. doi: 10.1093/cvr/cvp313

39. Ruiz-Villalba A, Simón AM, Pogontke C, Castillo MI, Abizanda G, Pelacho B, Sánchez-Domínguez R, Segovia JC, Prósper F, Pérez-Pomares JM (2015) Interacting resident epicardium-derived fibroblasts and recruited bone marrow cells form myocardial infarction scar. J Am Coll Cardiol 65:2057–2066. doi: 10.1016/j.jacc.2015.03.520

40. Smits A, Riley P (2014) Epicardium-Derived Heart Repair. J Dev Biol 2:84–100. doi: 10.3390/jdb2020084

41. Smits AM, Van Laake LW, Den Ouden K, Schreurs C, Szuhai K, Van Echteld CJ, Mummery CL, Doevendans PA, Goumans MJ (2009) Human cardiomyocyte progenitor cell transplantation preserves long-term function of the infarcted mouse myocardium. Cardiovasc Res 83:527–535. doi: 10.1093/cvr/cvp146

42. Takeichi M, Nimura K, Mori M, Nakagami H, Kaneda Y (2013) The Transcription Factors Tbx18 and Wt1 Control the Epicardial Epithelial-Mesenchymal Transition through Bi-Directional Regulation of Slug in Murine Primary Epicardial Cells. PLoS One. doi: 10.1371/journal.pone.0057829

43. van Wijk B, Gunst QD, Moorman AFM, van den Hoff MJB (2012) Cardiac Regeneration from Activated Epicardium. PLoS One. doi: 10.1371/journal.pone.0044692

44. Zhou B, Honor LB, He H, Qing M, Oh JH, Butterfield C, Lin RZ, Melero-Martin JM, Dolmatova E, Duffy HS, Von Gise A, Zhou P, Hu YW, Wang G, Zhang B, Wang L, Hall JL, Moses MA, McGowan FX, Pu WT (2011) Adult mouse epicardium modulates myocardial injury by secreting paracrine factors. J Clin Invest 121:1894–1904. doi: 10.1172/JCI45529

Supplementary figures

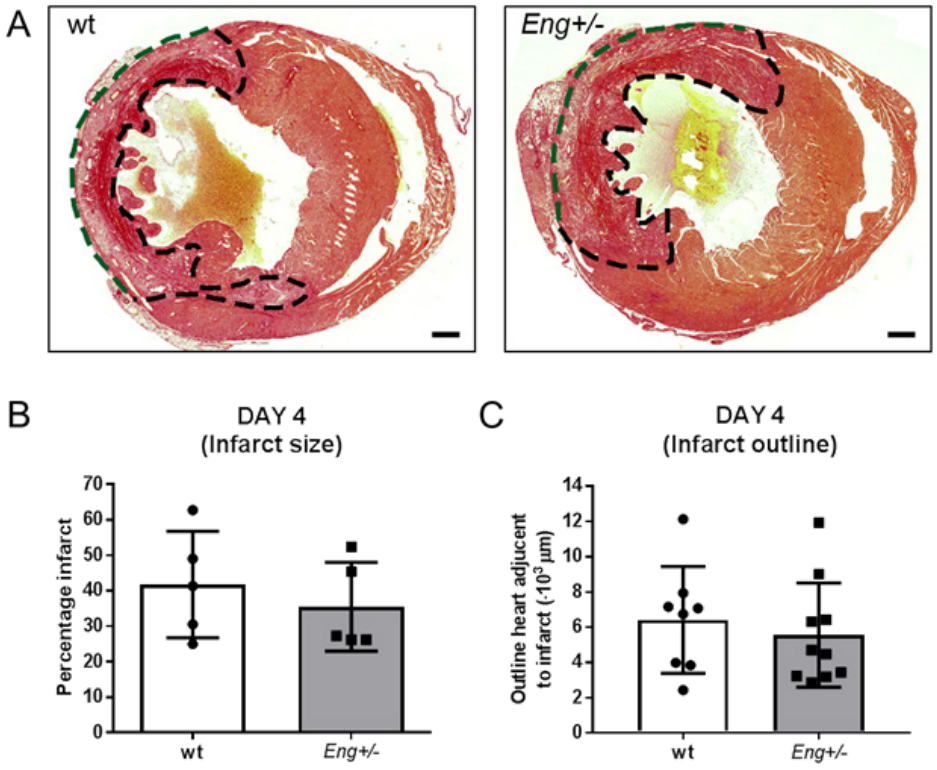

Supplementary Figure 1: Infarct size is equal between wt and Eng+/- hearts. A. In PSR stainings, the infarct area is outlined by a dashed line and the periphery of the infarct is indicated by a green dashed line. Scale bars: 500 µm. B,C. At 4 days post-MI, B. Wt and Eng+/- mice have an equal infarct size (n = 5 mice for each group). and C. no difference in the infarct periphery (n = 8-10 mice for each group)

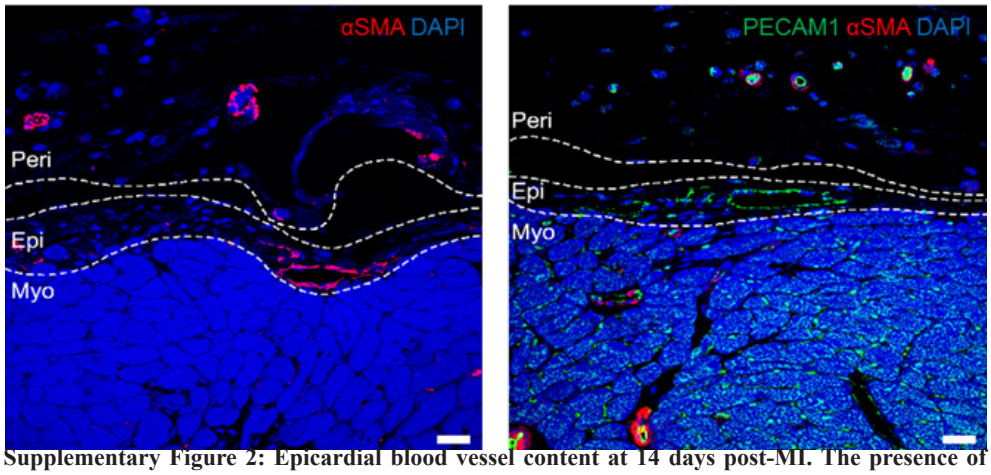

Supplementary Figure 2: Epicardial blood vessel content at 14 days post-MI. The presence of blood vessels within the epicardial border zone was quantified in alpha smooth muscle actin (αSMA) and platelet and endothelial cell adhesion molecule 1 (PECAM1) co-stainings. The dashed lines indicate the border between myocardium, (sub)epicardium and pericardium. Scale bars: 20 µm. Epi: (sub)epicardium, Myo: myocardium and Peri: pericardium

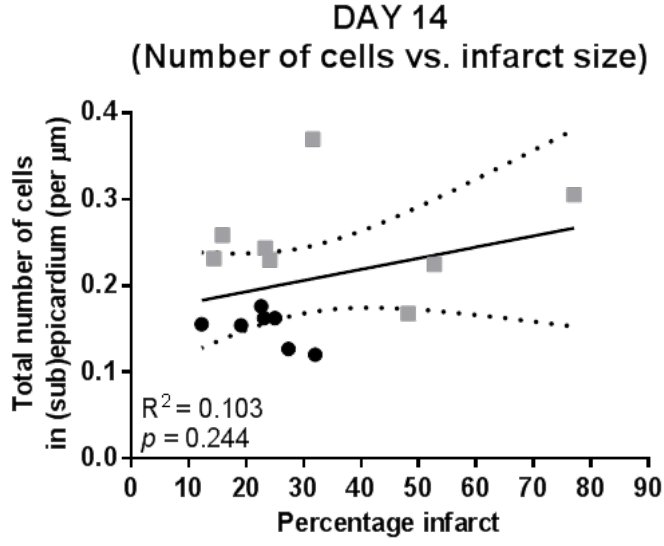

Supplementary Figure 3: Size of the epicardial border zone is not correlated with infarct size. Plotting the infarct size of wt and Eng+/- mice at day 14 post-MI against the number of cells within the epicardial border zone shows that there is no correlation. Eng+/- mice are depicted in grey/square data points (n = 7-8 mice for each group)

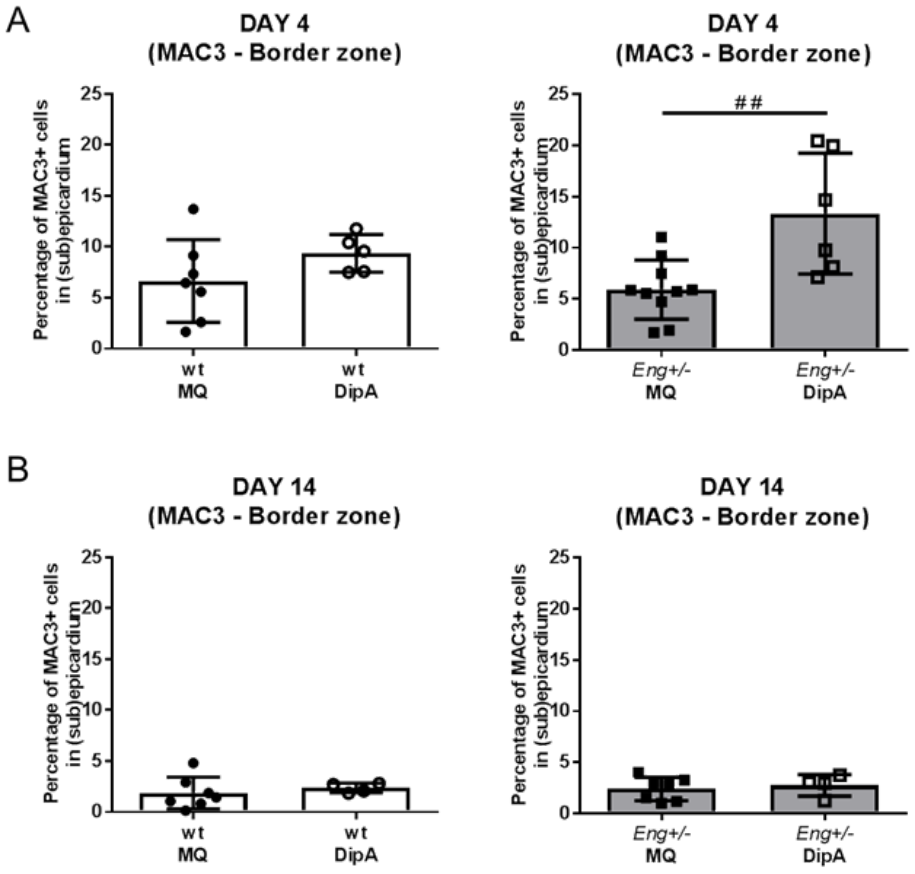

Supplementary Figure 4: Percentage of MAC3+ cells within the epicardial border zone upon DipA administration. A. MAC3+ cells in the (sub)epicardial border zone, 4 days post-MI. DipA treatment only significantly increases the percentage of MAC3+ cells within the Eng+/- epicardial border zone (n = 6-10 mice for each group). B. MAC3+ cells in the (sub)epicardial border zone, 14 days post-MI. At 14 days, no difference was observed in the percentage of MAC3+ cells within the epicardial border zone upon treatment for both wt and Eng+/- mice (n = 4-7 mice for each group). Data information: # #: p<0.01